Available online at www.sciencedirect.com
ScienceDirect
Journal of Catalysis 247 (2007) 129–136
JOURNAL OF CATALYSIS
www.elsevier.com/locate/jcat

# Introducing a new surface science model for Ziegler–Natta catalysts: Preparation, basic characterization and testing

Adelaida Andoni [a,b], John C. Chadwick [b,c], Stefania Milani [d], Hans (J.W.) Niemantsverdriet [a,b], Peter C. Thüne [a,b,*]

[a] *Schuit Institute of Catalysis, Eindhoven University of Technology, P.O. Box 513, 5600 MB Eindhoven, The Netherlands*
[b] *Dutch Polymer Institute (DPI), P.O. Box 902, 5600 AX Eindhoven, The Netherlands*
[c] *Laboratory of Polymer Chemistry, Eindhoven University of Technology, P.O. Box 513, 5600 MB Eindhoven, The Netherlands*
[d] *Dipartimento di Chimica, Università degli Studi di Ferrara, Via L. Borsari 46, 44100 Ferrara, Italy*

Received 11 December 2006; revised 22 January 2007; accepted 23 January 2007

Available online 2 March 2007

**Abstract**

An active model for a Ziegler–Natta ethylene polymerization catalyst has been prepared by spin-coating of a $MgCl_2$ solution in ethanol on a flat silicon (100) substrate covered by amorphous silica. The flat model approach facilitates characterization of the catalyst using surface spectroscopy and microscopy techniques. This model catalyst features a Ti/Mg atomic ratio of 0.15 and a primary $MgCl_2$ crystal size of about 15 nm. The flat model is active for ethylene polymerization, producing smooth polymer films. Scanning electron microscopy of these films reveals pillary polymer growth, in the direction perpendicular to the flat support surface.


*Keywords:* Model catalyst; Ziegler–Natta catalysis; Morphology; Atomic force microscopy; Scanning electron microscopy; X-ray photoelectron spectroscopy

## 1. Introduction

Ziegler–Natta catalytic systems are widely used in industrial olefin polymerization processes. They consist of a $MgCl_2$ support, $TiCl_4$, and an internal electron donor and are used in combination with an aluminum alkyl co-catalyst $AlR_3$ [1]. Lewis bases (external electron donors) are added in polymerization to produce highly isotactic polypropylene. One function of the internal electron donor—typically a monoester, diester or diether incorporated in the catalyst preparation—is to control the amount and distribution of $TiCl_4$ on the support surface. Giannini [2] has indicated that on the lateral cleavage surfaces of the $MgCl_2$ crystallites making up the support, the magnesium atoms are coordinated with 4 or 5 chlorine atoms, as opposed to 6 chlorine atoms in the bulk of the crystal. These tetracoordinated and pentacoordinated Mg atoms are present on the (110) and (100) lateral cuts of $MgCl_2$. Treatment with $TiCl_4$ will lead to adsorbed $TiCl_4$ species on one or both of the (100) and (110) cuts. On reaction with the co-catalyst ($AlR_3$), $Ti^{4+}$ is reduced to $Ti^{3+}$, and a Ti–C bond is introduced that is necessary for the insertion of the monomer.

Despite numerous efforts, questions regarding which $MgCl_2$ surface plane is the most preferred cut for $TiCl_4$ fixation, as well as what is the precise structure of the titanium active centers formed by treatment of the catalyst with the alkylaluminum co-catalyst, have still not been answered definitively. It has been suggested [3,4] that dimeric species ($Ti_2Cl_8$) epitactically coordinated to the (100) lateral cut could lead to the formation of stereospecific active sites. However, recent spectroscopic studies using FT-Raman have provided evidence for strong adsorption of $TiCl_4$ on the (110) lateral cut of $MgCl_2$, giving a monomeric species with octahedrally coordinated titanium, which can be the precursor for active and stereospecific sites [5,6]. Various attempts to characterize the active species in Ziegler–Natta catalysts have involved the use of advanced surface science techniques and model catalysts. Somorjai et

* Corresponding author. Fax: +31 40 247 3481.
*E-mail address:* p.c.thuene@tue.nl (P.C. Thüne).

0021-9517/$ – see front matter 
doi:10.1016/j.jcat.2007.01.019

al. have published a series of papers describing two synthetic routes to Ziegler–Natta model catalysts under UHV conditions. Ultra-thin films of $MgCl_2$ were prepared via sublimation onto a gold foil, followed by gas-phase deposition of $TiCl_4$, whereas $TiCl_4/TiCl_2$ films were obtained by $TiCl_4$ and Mg co-deposition on $MgCl_2$ and Au [7–12]. X-ray photoelectron spectroscopy (XPS) analysis revealed the presence of $TiCl_2Et$ species on the catalyst surface after exposure to the co-catalyst, $AlEt_3$. Prolonged reaction with $AlEt_3$ produced further reduced species with possible stoichiometry $TiClEt_n$ ($n = 1$ and/or 2). No evidence was found for $TiCl_3$ formation. It was suggested that $TiCl_4$ reduction and alkylation could not be separated under these experimental conditions [7–11]. The same group of authors reported the reduction of $MgCl_2$ by $AlEt_3$ in the presence of Au, forming Mg clusters or islands; a large fraction of the resulting support surface was capable of $TiCl_4$ chemisorption [13]. These systems were active for ethylene and propylene polymerization. The polymers produced were characterized by means of surface science techniques, atomic force microscopy, and vibrational spectroscopies and it was shown that polypropylene films had a high degree of isotacticity [14–16]. By alternating the supply of propylene and ethylene monomers, alternating polypropylene and polyethylene films were produced on one model Ziegler–Natta catalyst [17]. By means of this approach, it was shown that the active sites were present at the interface of the catalyst and the growing polymer and polymerization at the active sites occurred by the diffusion of monomers through the growing polymer layer. In the same framework, using the above models, temperature-programmed desorption (TPD) was used with physisorbed mesitylene as nondestructive surface probe to distinguish the surface adsorption sites of model Ziegler–Natta polymerization catalysts [18–20].

Following the work of Somorjai et al., Pilling et al. [21] reported the use of reflection absorption infrared spectroscopy (RAIRS) and XPS for a study of the interaction of $TiCl_4$ with metallic Mg films grown on an Au surface. Siokou and Ntais [22,23] introduced a surface science model of Ti-based Ziegler–Natta catalysts supported on $SiO_2/Si(100)$ and prepared by spin-coating THF solutions of $TiCl_4{\cdot}(THF)_2$ and $MgCl_2/TiCl_4{\cdot}(THF)_2$. The surface composition was characterized by XPS. Following the same approach, $TiCl_4{\cdot}(THF)_2$ was impregnated by spin-coating on a Si(100) wafer covered with a thin $SiO_x$ layer and on a polycrystalline Au foil [24]. Atomic force microscopy (AFM) measurements revealed a homogeneous distribution of nanosized $TiO_x$ clusters of semiellipsoid shape and increased contact area with the underlying silica. Fregonese et al. [25] reported XPS studies of Ziegler–Natta catalysts prepared by exposure of $\delta$-$MgCl_2$ to $TiCl_4$ and co-catalyst ($AlEt_3$) under UHV conditions, whereas Freund et al. [26] introduced a model system of a Pd(111) substrate covered by a $MgCl_2$ film onto which $TiCl_4$ was anchored and applied electron spin resonance to study intermediately formed radicals in Ziegler–Natta polymerization of ethylene. In addition, in more recent studies, Kaushik et al. [27] applied XPS to show that the productivity of a catalyst can be correlated to the dispersion of titanium atoms on the $MgCl_2$ support.

Following previous studies on surface science characterization of chromium species on flat silicon wafers [28–30], we aimed to develop a realistic flat model system for Ziegler–Natta catalysts that involves spin-coating of $MgCl_2$ from ethanol solution onto a silica wafer, followed by contact with $TiCl_4$ in toluene at room temperature. In this way we attempt to mimic an industrial catalyst preparation in which supports formed by cooling emulsions of molten $MgCl_2{\cdot}n$EtOH adducts in paraffin oil are reacted with $TiCl_4$ [1]. In this respect, we circumvent catalyst preparation under the UHV conditions used previously by other groups, which is often far removed from the nature of real industrial catalysts [22,25]. We used surface science and microscopy techniques, such as XPS, atomic force microscopy (AFM), and scanning electron microscopy (SEM), to study the surface chemistry and morphology of the support, catalyst and polymer. In this feasibility study, we demonstrate the construction of a realistic flat model of a Ziegler–Natta catalyst active for ethylene polymerization.

## 2. Experimental

### 2.1. Materials

Anhydrous magnesium chloride (beads, 99.9%), absolute ethanol (99.9%), titanium tetrachloride (99.9%), and triethyl aluminum (25 wt% in toluene) were purchased from Aldrich and used as received. HPLC-grade toluene was taken from an argon-flushed column packed with aluminum oxide and stored over 4 Å molecular sieves. Ethylene was supplied by Praxair (3.5).

### 2.2. Catalyst preparation and ethylene polymerization

The catalyst preparation is summarized in Scheme 1. All manipulations of air or water sensitive compounds were carried out using standard Schlenk or glovebox techniques. The $SiO_2/Si(100)$ wafer was prepared as described elsewhere (calcination at 750 °C, followed by etching with $H_2O_2/NH_3$) [28] to obtain an amorphous silica layer (20 nm) on a silicon (100) wafer. The wafer was partially dehydroxylated at 500 °C in air for 16 h. A small amount of surface hydroxyl groups was retained to facilitate a homogeneous $MgCl_2{\cdot}n$EtOH film formation. The wafer was then spin-coated with different concentrations of $MgCl_2$ in ethanol (2, 42, and 105 mmol/L). Spinning at 2800 rpm ejected most of the liquid from the flat silica surface, leaving behind a thin film of solution. The remaining solvent evaporated, and the solute precipitated on the support surface. The wafer was then dried under nitrogen and used for XPS and/or AFM analysis.

Grafting of $TiCl_4$ onto the $MgCl_2{\cdot}n$EtOH support was done by treatment with a 10% (v/v) $TiCl_4$ solution in toluene at room temperature. After washing with toluene to remove the physisorbed $TiCl_4$, the model catalyst was dried under nitrogen. Thus, the flat silica wafer containing the immobilized catalytic components could be used for either ethylene polymerization or XPS analysis. Both the $TiCl_4$ treatment and the washing step took 30 min unless stated otherwise.

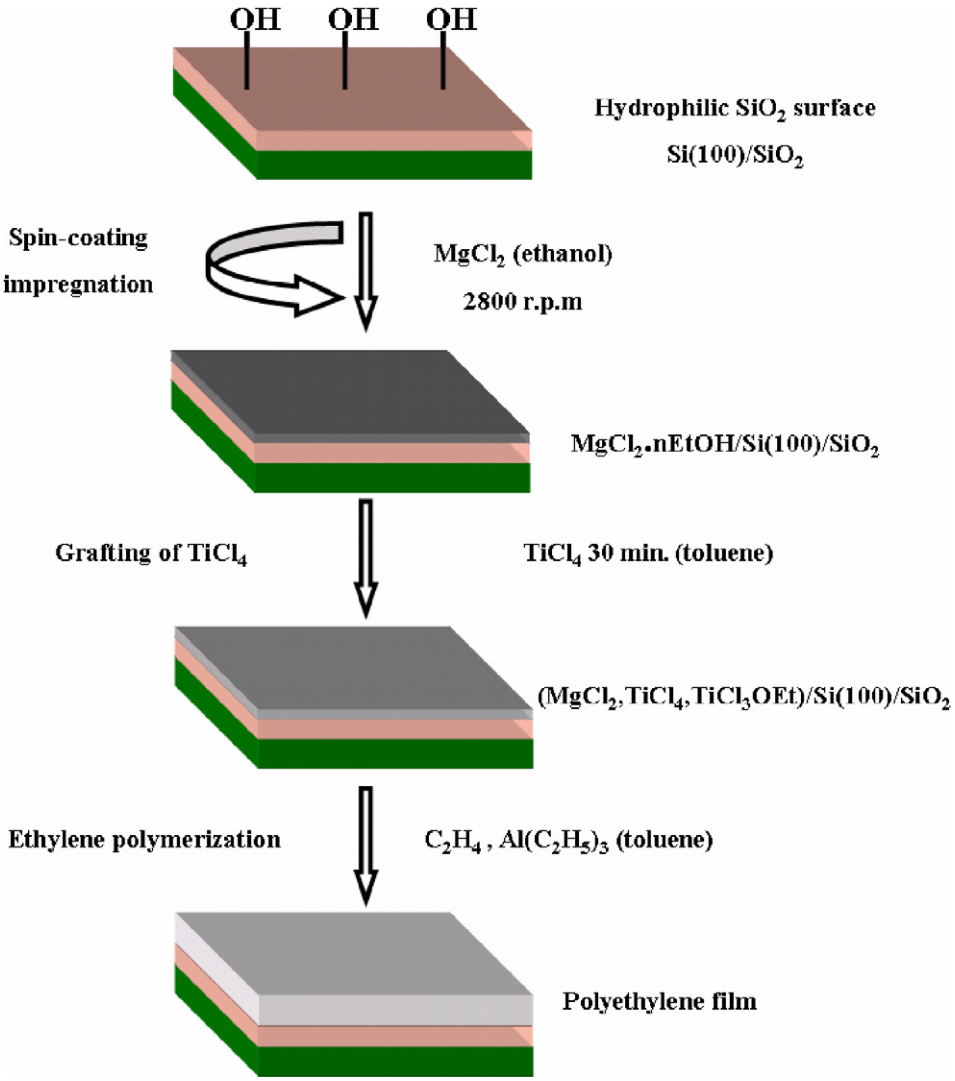


Scheme 1. Schematic representation of sample preparation for Ziegler–Natta catalyst on flat silica surface.

Ethylene polymerization was carried out at room temperature in a glass reactor equipped with a magnetic stirrer. The silica wafer after deposition of $MgCl_2{\cdot}n$EtOH and treatment with $TiCl_4$ was dipped into about 20 mL of a 1-mg/mL solution of the co-catalyst, $AlEt_3$, in toluene, inside the glass reactor. The reactor was pressurized with 2 bar of ethylene, and polymerization was allowed to run for the desired time. After polymerization, the wafer was washed with toluene.

### 2.3. Analytical techniques

AFM measurements were performed inside a glove box with Solver P47 base with SMENA head. The cantilever of choice was a noncontact gold-coated NSG11 (long end), manufactured by Micromasch. A typical tip force was 5.5 N/m, and a typical resonance frequency was 164 kHz. The measurements were performed in noncontact mode. The thickness of the catalyst support, $MgCl_2{\cdot}n$EtOH, was determined using the height difference between the Si substrate and $MgCl_2$ surface after scratching the layer with a scalpel.

The amounts of Mg in solution and on silica wafer were determined by an inductively coupled plasma optical emission spectrometry (ICP-OES) technique using a Spectro Circos CCD spectrometer. All solutions and the $MgCl_2$ of the spin-coated wafers were dissolved in $HCl_{aq}$ (0.1 M).

XPS measurements were performed with a VG Escalab 200 using a standard aluminum anode (Al$K\alpha$ 1486.3 eV) operating at 300 W. Spectra were recorded at normal emission background pressure, $1 \times 10^{-9}$ mbar. Binding energies were calibrated to a C 1s peak at 285 eV.

SEM was performed using a Philips environmental scanning electron microscope (XL-30 ESEM FEG; Philips, The Netherlands, now Fei Co.) in high-vacuum mode using a low accelerating voltage (low-voltage SEM) and a secondary detector.

Molecular weight and molecular weight distribution of the resulting polyethylene were determined by high-temperature gel permeation chromatography (GPC) in 1,2,4-trichlorobenzene at 140 °C using a PL 220 instrument and a calibration with polystyrene standards.

## 3. Results

### 3.1. Quantification of $MgCl_2$·*n*EtOH/$SiO_2$/Si(100)

The spin-coating of magnesium chloride as a solution in ethanol resulted in the formation of adducts of type $MgCl_2$·*n*EtOH on the surface of the silica wafer. The residual ethanol content depends on the conditions under which the wafer is dried after spin-coating, because $MgCl_2$·*n*EtOH adducts can be at least partially dealcoholized under relatively mild conditions [31]. The amounts of $MgCl_2$ on silica wafers were quantified with ICP. The amount of Mg on silica was scaled almost linearly with the concentration of the spin-coating solutions as the loading increased. Our standard catalyst used for ethylene polymerization was prepared from a 42 mmol/L solution, resulting in a Mg loading of 200 atoms/nm$^2$.

### 3.2. XPS analysis

The evolution of the $MgCl_2$·*n*EtOH film on the flat silica support was followed with XPS. On increasing the $MgCl_2$·*n*EtOH loading from 50 Mg atom/nm$^2$ to 200 and 400 Mg atom/nm$^2$, respectively, the corresponding signals Mg 2p, 2s and Cl 2p, 2s also increased in the overview spectra (Fig. 1a). The silica contributions Si 2p, 2s (Figs. 1a and 1b) diminished with increasing loading. As the Si peak became invisible, C 1s and O 1s remained significant in the spectra, likely due to the presence of residual ethanol in the spin-coated adduct $MgCl_2$·*n*EtOH. Unfortunately, however, the possible presence of adsorbed water and/or hydrocarbons (the latter present in the atmosphere of the glove box) prevented reliable quantification of the amount of residual ethanol (i.e., the value of *n* in $MgCl_2$·*n*EtOH). Angle-resolved XPS revealed that carbon and oxygen were present largely on top of the spin-coated film, whereas this would not be the case if the C and O were attributable solely to ethanol.

The Si 2s/Mg 2s ratio for our standard catalyst (200 Mg atoms/nm$^2$) was 0.17. This corresponds to a film thickness of about 11 ± 2 nm, assuming a flat homogeneous $MgCl_2$·*n*EtOH film over a large area [32,33]. The Mg/Cl ratio (1.00:1.96) closely resembled that of anhydrous $MgCl_2$, indicating that $MgCl_2$·*n*EtOH was deposited without any significant hydrolysis.

Treatment with $TiCl_4$ was carried out on a silica wafer with a loading of 200 Mg atoms/nm$^2$. The wafer was contacted for 30 min with a 10% (v/v) $TiCl_4$ solution in toluene, followed by a 30-min extraction with toluene to remove weakly bound $TiCl_4$. Fig. 2 displays overview spectra before and after the support was contacted with $TiCl_4$. The spectra show the Mg 2s and Si 2s peaks before and after the $TiCl_4$ treatment, together with the Ti 2p peak after the contact with $TiCl_4$. The Si/Mg ratio did not change on treatment with $TiCl_4$, indicating that the film remained largely intact and the film thickness remained constant. The Mg 2s and Mg 2p emissions showed maxima at BE 90.7 eV and 51.8 eV, whereas Cl $2p_{3/2}$ appeared at 199.5 eV. The maximum of the Ti $2p_{3/2}$ emission was at 459.3 eV, typical for $Ti^{4+}$. The Ti 2p/Mg 2s ratio of the $TiCl_4$/$MgCl_2$·*n*EtOH/$SiO_2$/Si(100) system corresponds to a Ti/Mg atomic ratio of 0.15 [34]. This ratio remained constant when the take-off angle for the photoelectrons was changed from 0° to 60° relative to the surface, indicating a homogeneous distribution of the Ti in the $MgCl_2$·*n*EtOH film.

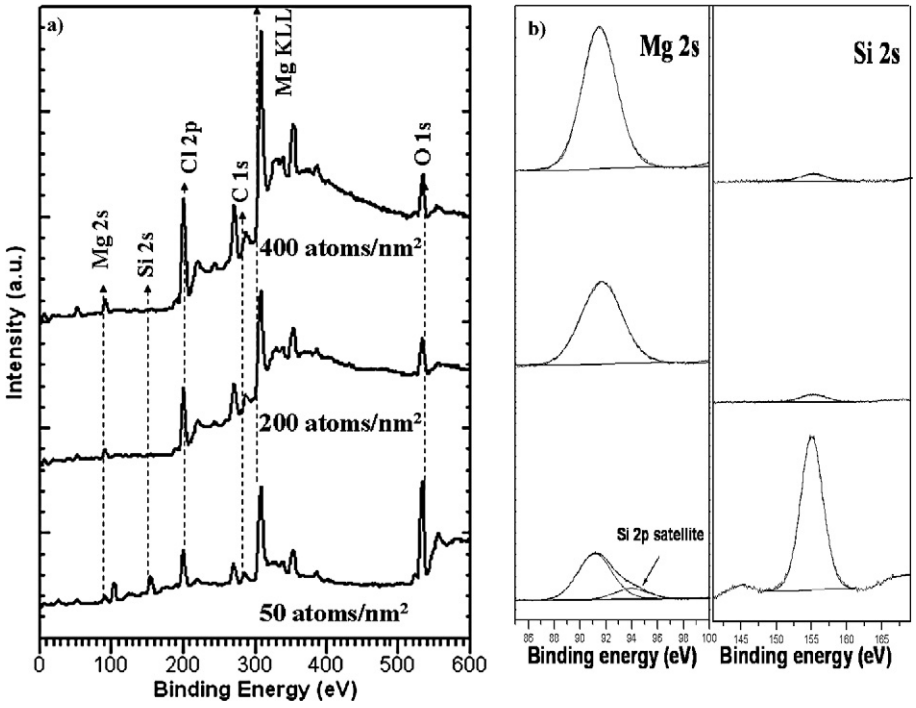


Fig. 1. (a) Wide scan of XPS spectra upon increasing the loading of $MgCl_2$·*n*EtOH on silica (from bottom to top the loading increases successively, i.e., 50, 200 and 400 atoms/nm$^2$); (b) XPS spectra of the same system recorded in the regions of Mg 2s and Si 2s for the same loadings.

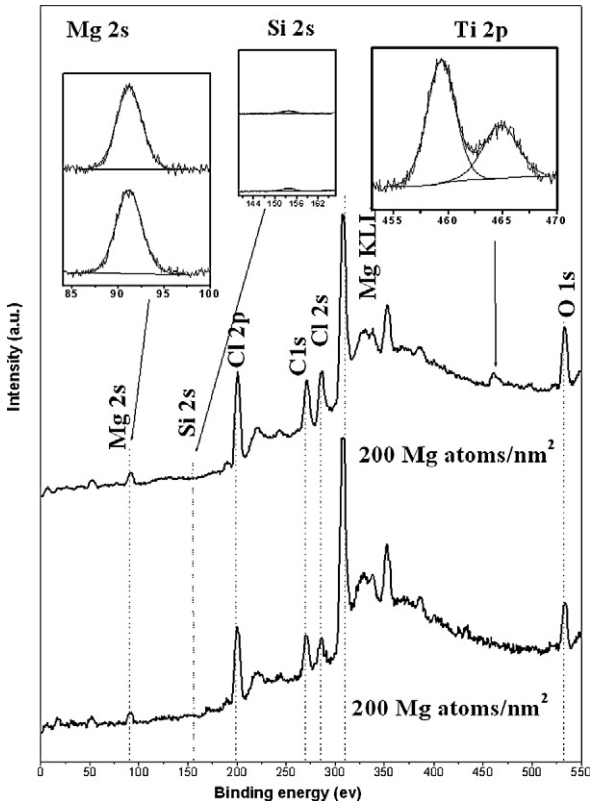


Fig. 2. Wide scan of XPS spectra before and after the $MgCl_2{\cdot}n$EtOH/$SiO_2$/Si(100) model support was treated with $TiCl_4$. The inserted spectra represent the Ti 2p peak after treatment with $TiCl_4$ and the Mg 2s and Si 2s peaks before and after treatment with $TiCl_4$.

The Ti $2p_{3/2}$ peak appeared slightly broader after contact with $AlEt_3$. The FWHM was 4.1 eV, compared with 3.0 eV before alkylation. The increased width of the Ti $2p_{3/2}$ peak after reaction with the co-catalyst indicates some reduction to oxidation states lower than 4+, although a well-resolved peak for titanium atoms in lower oxidation state was not evident.

### 3.3. AFM analysis

The morphology of the $MgCl_2{\cdot}n$EtOH support with a $MgCl_2$ loading of 200 atoms/nm$^2$ was probed with AFM before and after treatment with $TiCl_4$. The spin-coated $MgCl_2$ (in ethanol) yielded a smooth film with a surface roughness of 1–3 nm (Fig. 3). At high magnification, the AFM image indicated a granular structure. The grain size varied between 10 and 40 nm. Fig. 4a represents the scratching of a typical $MgCl_2{\cdot}n$EtOH film (200 Mg atoms/nm$^2$) with the corresponding height profile. The film thickness was proportional to the loading of the Mg on silica (Fig. 4b). Our standard loading (200 atoms/nm$^2$) corresponded to a film thickness of $12 \pm 2$ nm, in excellent agreement with the XPS results.

Treatment of the $MgCl_2{\cdot}n$EtOH film with $TiCl_4$ for 30 min induced minor changes in morphology (Fig. 5a). The film thickness remained constant after the $TiCl_4$ treatment. AFM (Fig. 5a) showed a homogeneous film with some small holes with a penetration depth of several nm. These holes possibly could have resulted from detachment of small grains of magnesium chloride from the wafer surface, as shown in the higher-resolution image in Fig. 3. This effect is more pronounced at longer treatments with $TiCl_4$ (e.g., 18 h). Fig. 5b shows the formation of larger holes with a penetration depth up to $\pm 12$ nm.

### 3.4. Ethylene polymerization

The model catalyst prepared as described above proved to be active for ethylene polymerization at 2 bar ethylene pressure and room temperature. PE is formed, in milligram quantities, as a thin film on the silica surface ($3 \times 3$ cm$^2$). No polymer formation was observed in the solution. SEM indicated a polymer film thickness of 4 μm after 30 min of polymerization and 100 μm after 16 h of polymerization. This corresponds to a polymer yield of 3.5 kg PE/g $MgCl_2$ after 16 h. In the SEM images (Fig. 6), the polymer films appear to consist of a mass of spherical particles when viewed from the top; however, a lateral view clearly reveals that the polymer films consist of closely packed pillars aligned perpendicular to the surface of the support, indicating a vertical growth of the polyethylene film. The polymer obtained after 16 h of polymerization had an $M_w$ of $2.5 \times 10^6$ g/mol and a molecular weight distribution ($M_w/M_n$) of 4.4.

## 4. Discussion

A flat model catalyst prepared by spin-coating of $MgCl_2{\cdot}n$EtOH from ethanol solution onto a flat silicon wafer and subsequent treatment with $TiCl_4$ was studied by XPS, AFM, and SEM, with the aim of characterizing and visualizing the Ziegler–Natta catalyst as well as the polymer produced. Our model resembles industrial counterparts in several aspects. AFM in combination with XPS showed that the thickness of the $MgCl_2{\cdot}n$EtOH film can be tuned by varying the loading of Mg on Si. The spin-coating of $MgCl_2{\cdot}n$EtOH yielded smooth films consisting of grains ranging in size from 10 to 40 nm, not very different from the size of primary particles in industrial Ziegler–Natta catalysts [35–37]. The density of the $MgCl_2{\cdot}n$EtOH film prepared at our standard loading was ∼14 atoms/nm$^3$, close to the density of anhydrous $MgCl_2$ (∼15 atoms/nm$^3$).

On treatment of the $MgCl_2{\cdot}n$EtOH/$SiO_2$/Si(100) model support with $TiCl_4$, the spin-coated film remained largely intact. AFM revealed only minor effects on morphology and no change in the layer thickness. The Ti/Mg ratio was ∼0.15 according to XPS analysis. Ti was distributed homogeneously in the film. In earlier work, Magni and Somorjai [7] reported a Ti/Mg ratio of ∼0.2–0.8 with increasing exposure of their model $MgCl_2$ film to $TiCl_4$, whereas Kaushik et al. [27] reported a Ti/Mg ratio of ∼0.12–0.29 for Ziegler–Natta catalysts. Ti/Mg ratios of around 0.04–0.15 are typical for Ziegler–Natta catalysts used for polypropylene [38]. The chemical state of the $TiCl_4$ in our model catalyst remains ambiguous. The binding energy of 459.3 eV is typical for $Ti^{4+}$ and is close to that of $TiO_2$. During the reaction of the spin-coated support precursor

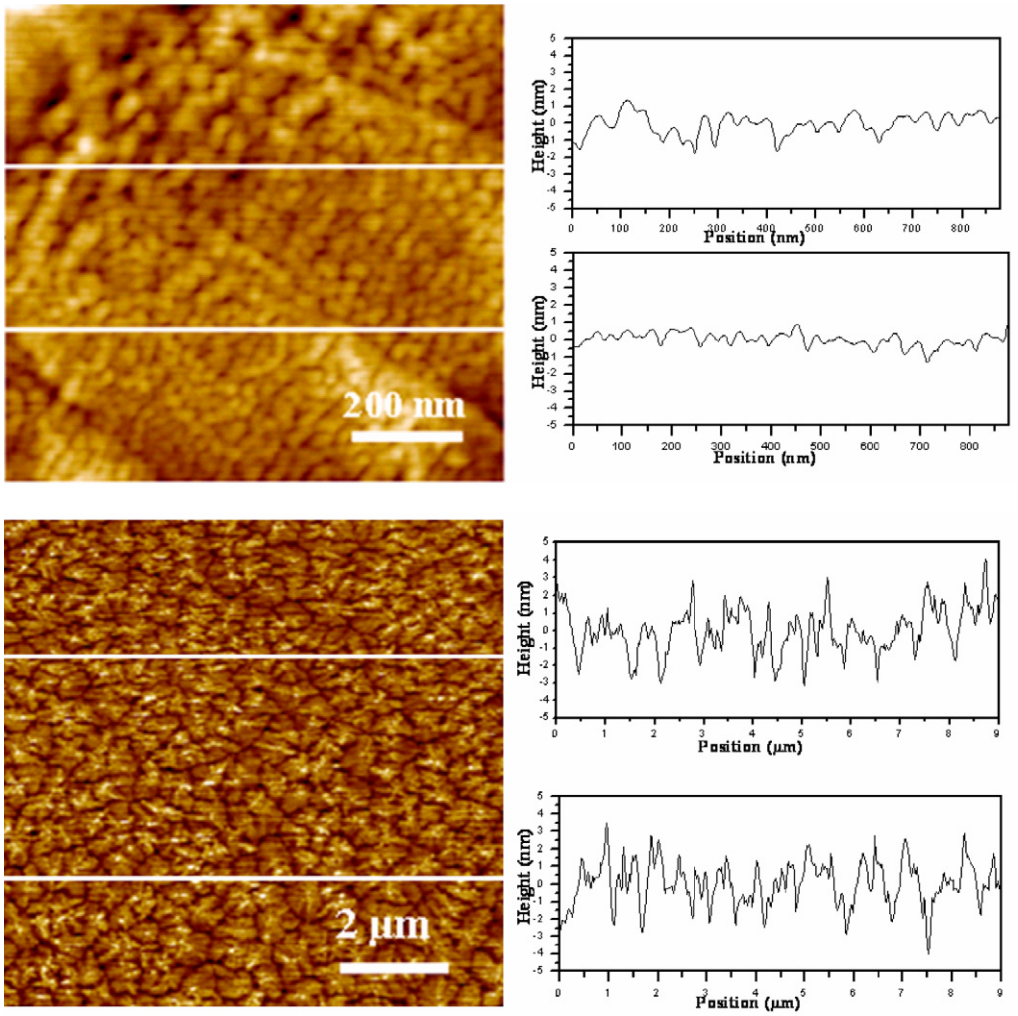


Fig. 3. (Left) AFM height images of $MgCl_2{\cdot}n$EtOH film for loading of 200 atoms/nm$^2$ on silica; (right) the corresponding cross-sectional height scans.

($MgCl_2{\cdot}n$EtOH) with $TiCl_4$, compounds of type $TiCl_{4-n}(OEt)_n$ are formed. Removal and replacement of such species by $TiCl_4$ is relatively difficult [35] and they likely are present in this model system despite the large excess of $TiCl_4$ in the catalyst preparation.

The $MgCl_2{\cdot}n$EtOH/$SiO_2$/Si(100) model catalyst polymerized ethylene in the presence of $AlEt_3$ after treatment with $TiCl_4$. We were able to produce a polyethylene layer 10,000 times thicker than the spin-coated support layer (100 μm thick PE, as opposed to the $12 \pm 2$ nm of support $MgCl_2$). SEM indicated the formation of a 4-μm layer of polyethylene after 30 min and a 100-μm layer after 16 h. The final polyethylene yield after 16 h was 3.5 kg/g $MgCl_2$. This was obtained under very mild conditions (i.e., room temperature, 2 bar ethylene pressure). Magni and Somorjai [9,11] reported that titanium chloride systems formed by both electron irradiation-induced and metallic Mg-induced chemical vapor deposition on thin films of Au and $MgCl_2$ were active for ethylene polymerization under UHV conditions with a nominal monomer insertion rate of 1.3 $C_2H_4$ molecules/(Ti atom) s at 760 Torr and 300–350 K. Our system has a nominal insertion rate of 1.4 $C_2H_4$ molecules/(Ti atom) s at 2 bar and room temperature.

## 5. Conclusion

Model Ziegler–Natta catalysts, active in ethylene polymerization, can be prepared by the spin-coating of $MgCl_2{\cdot}n$EtOH from ethanol solution onto a flat silica wafer, followed by contact with $TiCl_4$. The flat model approach is beneficial in many ways. It allows a surface chemistry and morphologic study of the catalyst and nascent polymer at the nanometer scale at each stage of catalyst preparation and polymerization, using electron and scanning probe microscopy as well as surface science techniques such as XPS.

The catalyst preparation method is relevant for industrial Ziegler–Natta catalysts and produces $MgCl_2{\cdot}n$EtOH grains, which, according to AFM observations, range in size from 10 to a few tens of nm. Treatment of $MgCl_2{\cdot}n$EtOH with $TiCl_4$ results in a homogeneous distribution of Ti and Ti/Mg ratios similar to those in industrial catalysts. The model catalyst, together with $AlEt_3$ as a co-catalyst, shows reasonable

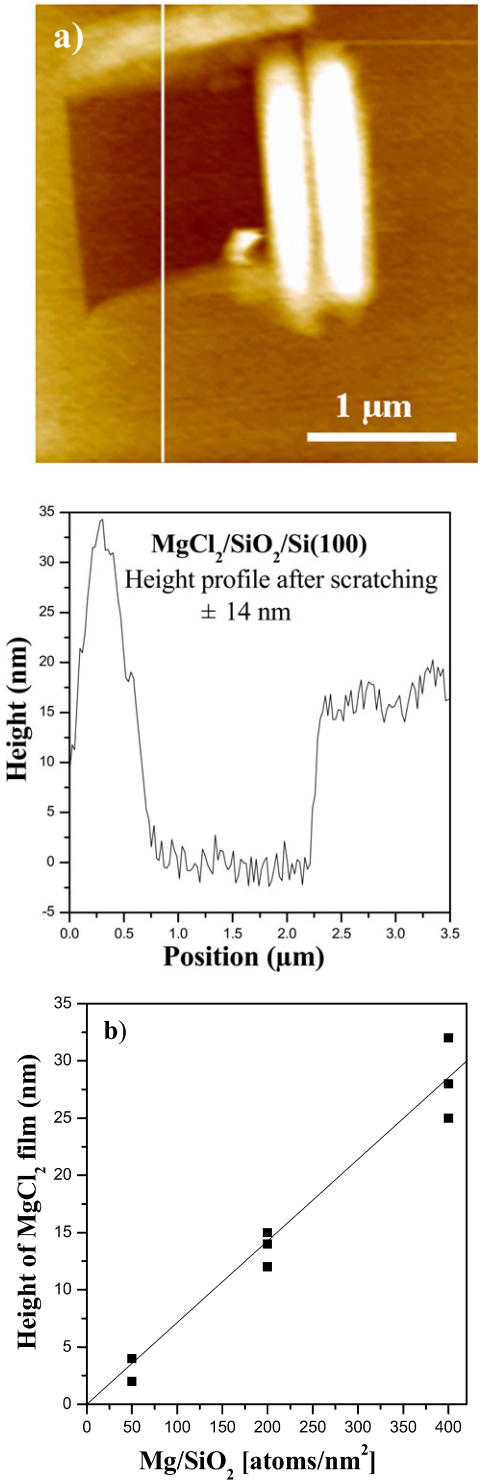


Fig. 4. (a) $MgCl_2 \cdot n$EtOH film on Si after scratching and the corresponding cross-sectional height scan (200 Mg atoms/$nm^2$); (b) thickness of $MgCl_2$ films vs the loading of Mg.

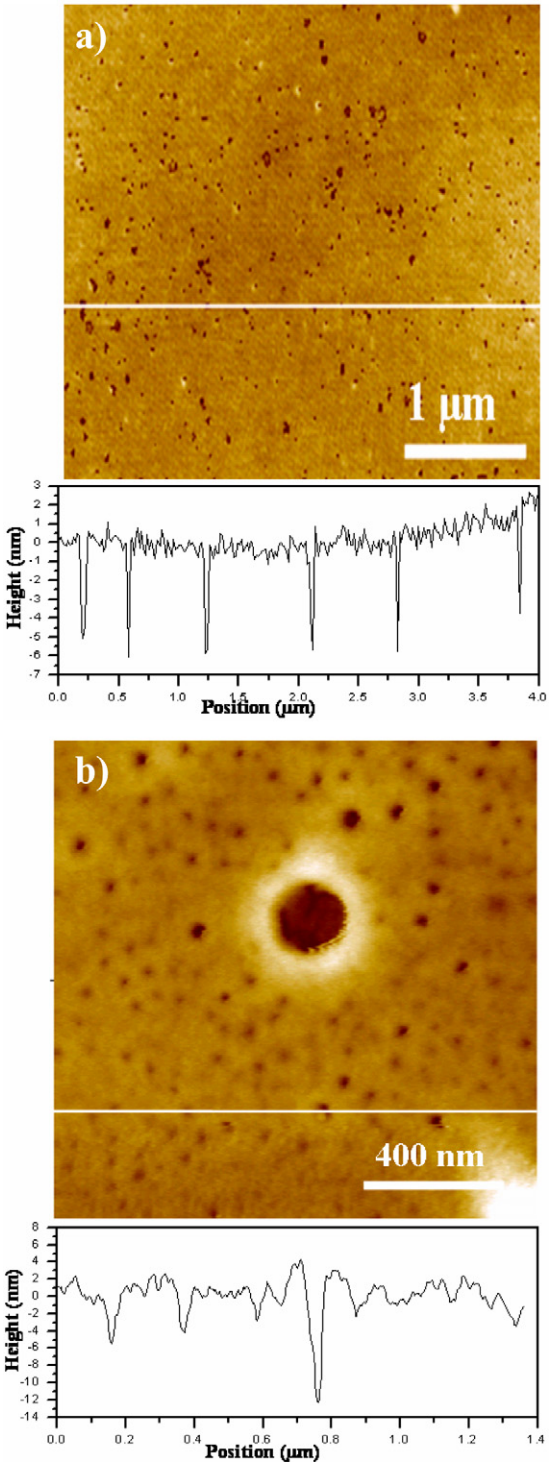


Fig. 5. (a) AFM height image after treatment of $MgCl_2 \cdot n$EtOH film (200 Mg atoms/$nm^2$) with $TiCl_4$ for 30 min, with the corresponding cross-sectional height scans; (b) AFM images after treatment of a similar film with $TiCl_4$ for 18 h, with the corresponding cross-sectional height scans.

activity in ethylene polymerization, with polymer growth occurring perpendicular to the flat support surface. We are currently extending this approach to the preparation and characterization of well-defined crystallites of $MgCl_2$ on flat silicon wafers, including an investigation of how the formation of different crystallite faces of $MgCl_2$ is affected by the Lewis bases used as internal donors in Ziegler–Natta catalysts for polypropylene. We also plan to apply in situ ATR-infrared spectroscopy to gain further insight into the $MgCl_2 \cdot n$EtOH support composition and the effect of $TiCl_4$ and donor adsorption on the support on stereoselectivity during propylene polymerization.

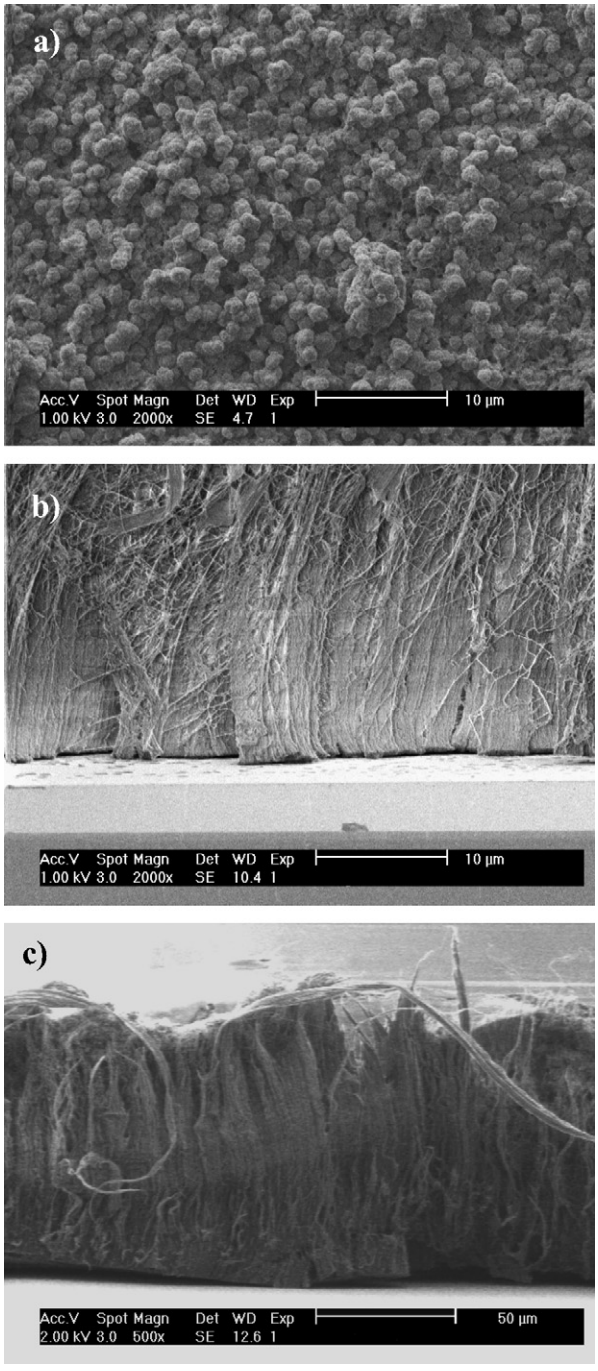


Fig. 6. SEM image of polyethylene obtained after 16 h polymerization: (a) top view, (b) and (c) side view on silica wafer.

## Acknowledgments

This research forms part of the research program of the Dutch Polymer Institute (DPI) under Project 387. The authors thank V. Grumel, University of Stellenbosch, South Africa, for the GPC analyses; A.M. Elemans-Mehring, Eindhoven University of Technology, The Netherlands, for the ICP measurements; and D. Ovchinnikov, Eindhoven University of Technology, and A.M. Alexeev, State Research Institute of Physical Problems, Russia, for the AFM measurements.

## References

[1] E. Albizzati, G. Cecchin, J.C. Chadwick, G. Collina, U. Giannini, G. Morini, L. Noristi, in: N. Pasquini (Ed.), Polypropylene Handbook, second ed., Hanser, Munich, 2005, chap. 2.
[2] U. Giannini, Makromol. Chem. Suppl. 5 (1981) 216.
[3] P. Corradini, V. Busico, G. Guerra, in: W. Kaminsky, H. Sinn (Eds.), Transition Metals and Organometallics as Catalysts for Olefin Polymerization, Springer-Verlag, Berlin, 1988, p. 337.
[4] V. Busico, P. Corradini, L. De Martino, A. Proto, V. Savino, E. Albizzati, Makromol. Chem. 186 (1985) 1279.
[5] L. Brambilla, G. Zerbi, S. Nascetti, F. Piemontesi, G. Morini, Macromol. Symp. 213 (2004) 287.
[6] L. Brambilla, G. Zerbi, F. Piemontesi, S. Nascetti, G. Morini, J. Mol. Catal. A Chem. 263 (2007) 103.
[7] E. Magni, G.A. Somorjai, J. Phys. Chem. B 102 (1998) 8788.
[8] E. Magni, G.A. Somorjai, Surf. Sci. 345 (1996) 1.
[9] E. Magni, G.A. Somorjai, Surf. Sci. 377–379 (1997) 824.
[10] E. Magni, G.A. Somorjai, Surf. Sci. 341 (1995) L1078.
[11] T.I. Koranyi, E. Magni, G.A. Somorjai, Top. Catal. 7 (1999) 179.
[12] S.H. Kim, G.A. Somorjai, J. Phys. Chem. B 104 (2000) 5519.
[13] E. Magni, T.I. Koranyi, G.A. Somorjai, Langmuir 16 (2000) 8113.
[14] S.H. Kim, G.A. Somorjai, Surf. Interface Anal. 31 (2001) 701.
[15] E. Magni, G.A. Somorjai, Catal. Lett. 35 (1995) 205.
[16] S.H. Kim, G.A. Somorjai, J. Phys. Chem. B 106 (2002) 1386.
[17] S.H. Kim, G.A. Somorjai, Catal. Lett. 68 (2000) 7.
[18] S.H. Kim, C.R. Tewell, G.A. Somorjai, Langmuir 16 (2000) 9414.
[19] S.H. Kim, G.A. Somorjai, Appl. Surf. Sci. 161 (2000) 333.
[20] S.H. Kim, G.A. Somorjai, J. Phys. Chem. B 105 (2001) 3922.
[21] M.J. Pilling, A.A. Fonseca, M.J. Cousins, K.C. Waugh, M. Surman, P. Gardner, Surf. Sci. 587 (2005) 78.
[22] A. Siokou, S. Ntais, Surf. Sci. 540 (2003) 379.
[23] A. Siokou, S. Ntais, Surf. Sci. 600 (2006) 4216.
[24] S. Ntais, V. Dracopoulos, A. Siokou, J. Mol. Catal. A Chem. 220 (2004) 199.
[25] D. Fregonese, A. Glisenti, S. Mortara, G.A. Rizzi, E. Tondello, S. Bresadola, J. Mol. Catal. A Chem. 178 (2002) 115.
[26] H.-J. Freund, M. Bäumer, J. Libuda, T. Risse, G. Rupprechter, S. Shaikhutdinov, J. Catal. 216 (2003) 223.
[27] V.K. Kaushik, V.K. Gupta, D.G. Naik, Appl. Surf. Sci. 253 (2006) 753.
[28] P.C. Thüne, C.P.J. Verhagen, M.J.G. van den Boer, J.W. Niemantsverdriet, J. Phys. Chem. B 101 (1997) 8559.
[29] P.C. Thüne, J. Loos, A.M. de Jong, P.J. Lemstra, J.W. Niemantsverdriet, Top. Catal. 13 (2000) 67.
[30] E.M.E. van Kimmenade, A.E.T. Kuiper, Y. Tamminga, P.C. Thüne, J.W. Niemantsverdriet, J. Catal. 223 (2004) 134.
[31] J.C.J. Bart, W. Roovers, J. Mater. Sci. 30 (1995) 2809.
[32] J.H. Scofield, J. Electron. Spectrosc. Relat. Phenom. 8 (1976) 129.
[33] P.J. Cumpson, M.P. Seah, Surf. Interface Anal. 25 (1997) 430.
[34] J.F. Moulder, W.F. Stickle, P.E. Sobol, K.D. Bomben, in: J. Chastain (Ed.), Handbook of X-Ray Photoelectron Spectroscopy and Physical Electronics, Perkin–Elmer Co., Eden Prairie, MN, 1992.
[35] J.C. Chadwick, Ziegler–Natta Catalysts, Encyclopedia of Polymer Science and Technology, vol. 6, 2003, p. 517.
[36] H. Mori, M. Sawada, T. Higuchi, K. Hasebe, N. Otsuka, M. Terano, Macromol. Rapid Commun. 20 (1999) 245.
[37] L.L. Böhm, Angew. Chem. Int. Ed. 42 (2003) 5010.
[38] A.K. Yaluma, P.J.T. Tait, J.C. Chadwick, J. Polym. Sci. Part A Polym. Chem. 44 (2006) 1635.